

两个基于依诺沙星的稀土配合物的合成、晶体结构、 与 DNA 作用和抗菌活性

邓记华 梅光泉*

(江西省高等学校应用化学与化学生物学重点实验室, 宜春学院化生学院, 宜春 336000)

摘要: 通过溶剂热-溶液挥发法合成得到了 2 个基于依诺沙星(HEX)的稀土配合物 $[\text{Ce}(\text{Ex})_4] \cdot 39\text{H}_2\text{O}$ (**1**)和 $[\text{Sm}_2(\text{Ex})_4(\text{HEX})_2(\text{ox})] \cdot 24\text{H}_2\text{O}$ (**2**), 并运用红外光谱、元素分析和 X-射线单晶衍射等研究手段表征了它们的结构。研究表明: 配合物 **1** 为单核配合物; 配合物 **2** 为双核配合物。紫外滴定和荧光滴定研究结果表明: 它们均能以插入的方式作用于小牛胸腺 DNA, 结合常数(K_b)分别为 4.45×10^4 和 $6.56 \times 10^4 \text{ mol}^{-1} \cdot \text{L}$; 抗菌实验结果表明它们对革兰氏菌和真菌的活性均要优于依诺沙星配体本身。

关键词: 依诺沙星; 稀土配合物; 晶体结构; DNA 作用; 抗菌活性

中图分类号: O614.33*2; O614.33*7

文献标识码: A

文章编号: 1001-4861(2012)11-2431-06

Two Rare Earth Complexes Based on Enoxacin: Synthesis, Crystal Structures, DNA Binding and Antibacterial Activities

DENG Ji-Hua MEI Guang-Quan*

(College of Chemistry and Bio-engineering, Key Laboratory of Jiangxi University for Applied
Chemistry and Chemical Biology, Yichun University, Yichun, Jiangxi 336000, China)

Abstract: Two rare earth complexes based on enoxacin (HEX), $[\text{Ce}(\text{Ex})_4] \cdot 39\text{H}_2\text{O}$ (**1**) and $[\text{Sm}_2(\text{Ex})_4(\text{HEX})_2(\text{ox})] \cdot 24\text{H}_2\text{O}$ (**2**) (HEX=enoxacin; ox=oxalate), have been synthesized and characterized by IR, EA and X-ray diffraction. The analyses of the single X-ray diffraction results indicate that **1** is a mononuclear Ce(IV) complex and crystallizes in tetragonal system, space group $I4_1/a$ with $a=1.551\ 74(12) \text{ nm}$, $c=4.066\ 6(4) \text{ nm}$, $V=9.791\ 9(14) \text{ nm}^3$, $Z=4$, $\mu=0.574 \text{ mm}^{-1}$, $F(000)=4\ 480$, $D_c=1.441 \text{ g} \cdot \text{cm}^{-3}$, $R_1=0.074\ 3$, $wR_2=0.180\ 0$; **2** is an oxalate-bridged binuclear Sm(III) complex and crystallizes in triclinic system, space group $P\bar{1}$ with $a=1.505\ 72(19) \text{ nm}$, $b=1.511\ 98(10) \text{ nm}$, $c=1.610\ 58(10) \text{ nm}$, $\alpha=116.723(2)^\circ$, $\beta=107.987(2)^\circ$, $\gamma=98.020(2)^\circ$, $V=2.943\ 0(5) \text{ nm}^3$, $Z=1$, $\mu=1.095 \text{ mm}^{-1}$, $F(000)=1\ 412$, $D_c=1.545 \text{ g} \cdot \text{cm}^{-3}$, $R_1=0.039\ 4$, $wR_2=0.121\ 7$. The bindings of **1** and **2** with calf thymus DNA (CT-DNA) have been investigated by electronic absorption spectroscopy and emission spectroscopy. The results indicate that both complexes bind with double-stranded CT-DNA mostly via intercalative mode, with the intrinsic binding constants (K_b) of 4.45×10^4 and $6.56 \times 10^4 \text{ mol}^{-1} \cdot \text{L}$, respectively. Antibacterial tests show both complexes have better antibacterial activities against Gram and fungi microbial than the free ligand HEX. CCDC: 751128, **1**; 751129, **2**.

Key words: enoxacin; rare earth complex; crystal structure; DNA binding; antibacterial activity

The study on the interaction of small metal coordination molecules with DNA is of great importance because it can provide important reference in the design of new and more efficient anti-cancer drugs.

收稿日期: 2011-12-06。收修改稿日期: 2012-06-12。

江西省自然(青年)科学基金(No.2010GZH0126), 江西省教育厅科技计划(No.GJJ09637, GJJ12577, GJJ11603, GJJ10701)资助项目。

*通讯联系人。E-mail: djhyu_2006@yahoo.com.cn, yc_mgq@163.com

Over the past decades, a variety of transition metal complexes, especially Cu(II), Ru(II), and Pt(II) complexes have been synthesized and studied for their interactions with DNA^[1-3]. Although recent researches show rare earth complexes have good biological activities on antibacterial, anti-inflammation, and sterilization^[4], the report of their interactions to DNA are very limited^[5].

Enoxacin (HEx) is an important type of quinolone antibacterial agent^[6]. It can penetrate into bacterial cells and then to inhibit activity of DNA gyrase^[7]. In this process, the HEx molecule bonding to a metal is considered as an important step^[8]. Therefore, it is meaningful to investigate the interaction between its metal complex and DNA. In this paper, we present two HEx-based rare earth complexes, [Ce(Ex)₄]·39H₂O (**1**) and [Sm₂(Ex)₄(HEx)₂(ox)]·24H₂O (**2**). Their synthesis, characterization, binding with CT-DNA, and antibacterial activity are investigated and discussed.

1 Experimental

1.1 Syntheses

1.1.1 Ce(Ex)₄·39H₂O (**1**)

The mixture of Ce(NO₃)₃·6H₂O (1 mmol), HEx (2 mmol), and C₂H₅OH/H₂O (16 mL, V/V 1:1) was placed in a 25 mL Teflon-lined reactor and heated at 110 °C in an oven for 6 d. After cooled to room temperature, the resulting solution was filtered and the filtrate was allowed to stand at room temperature. Well-shaped light yellow crystals suitable for X-rays diffraction were obtained after one month with a yield of 53.6% based on HEx. Anal. Found(%): C, 34.06; H, 6.64; N, 10.51. Calcd. for C₆₀H₁₄₂F₄N₁₆O₅₁Ce (%): C, 33.99; H, 6.75; N, 10.57. IR (KBr): ν (cm⁻¹) 3 396(s), 2 773(w), 1 629(s), 1 579(s), 1 474(s), 1 446(s), 1 381(s), 1 369(s), 1 288(m), 1 256(m), 1 182(m), 1 128(w), 968(w), 825(m), 810(w), 752(m), 638(w), 627(m), 566(w), 528(w), 473(w).

1.1.2 [Sm₂(Ex)₄(HEx)₂(ox)]·24H₂O (**2**)

The mixture of SmCl₃·6H₂O (1 mmol), HEx (2 mmol), Na₂C₂O₄ (0.5 mmol), NH₃·H₂O (1 mL), and C₂H₅OH/H₂O (16 mL, V/V 1:1) was placed in a 25 mL Teflon-lined reactor and heated at 120 °C for 7 d. After cooled to room temperature, the resulting

solution was filtered and the filtrate was left to stand at room temperature. Well-shaped light yellow crystals suitable for X-rays diffraction were obtained after two weeks with a yield of 61.7% based on HEx. Anal. Found (%): C, 40.21; H, 5.43; N, 12.28. Calcd. for C₉₂H₁₄₆F₆N₂₄O₄₆Sm₂(%): C, 40.34; H, 5.37; N, 12.27. IR (KBr): ν (cm⁻¹) 3 422(s), 2 849 (w), 1 625(s), 1 607(s), 1 568(s), 1 474(s), 1 445(s), 1 367(m), 1 275(s), 1 255(m), 1 143(w), 1 114(m), 1 092(w), 943(w), 822(s), 790(w), 742(m), 683(w), 642(m), 503(w).

1.2 X-ray structure determination

Single-crystal data for **1** and **2** were collected at 173 K on a Bruker Smart 1000 CCD diffractometer, with Mo K α radiation (λ =0.071 073 nm), the empirical absorption corrections were applied using the SADABS program^[9]. Both structures were solved using direct methods, which yielded the positions of all non-hydrogen atoms. These were refined first isotropically and then anisotropically. All the hydrogen atoms of the ligands were placed in calculated positions with fixed isotropic thermal parameters and included in the structure factor calculations in the final stage of full-matrix least-squares refinement. The hydrogen atoms of lattice H₂O molecules in 1/2 were not assigned. All calculations were performed using the SHELXTL system of computer programs^[10]. The crystallographic data are summarized in Table 1.

CCDC: 751128, **1**; 751129, **2**.

1.3 Binding with CT-DNA

UV-Vis spectra of **1/2** in the absence and presence of CT-DNA were recorded on Varian Cary-100 UV-Vis spectrometer at room temperature. The absorption titrations of both complexes in buffer (5 mmol·L⁻¹ Tris-HCl, 50 mmol·L⁻¹ NaCl, pH 7.2) were performed by fixing the complex concentration to which increments of the DNA stock solution were added, respectively. Both complex solutions employed were 20 μ mol·L⁻¹ in concentration, to which CT-DNA was added at a certain ratio $c_{\text{DNA}}/c_{\text{complex}}$. Complex-DNA solutions were allowed to incubate for 10 min before the absorption spectra were scanned at the range of 190~500 nm.

The interactions of the complexes **1/2** with CT-

Table 1 Crystal data and structure refinements for **1** and **2**

Complex	1	2
Formula	C ₆₀ H ₁₄₂ F ₄ N ₁₆ O ₅₁ Ce	C ₉₂ H ₁₄₆ F ₆ N ₂₄ O ₄₆ Sm ₂
Formula weight	2 120.02	2 739.03
Crystal system	Tetragonal	Triclinic
Space group	<i>I</i> 4 ₁ / <i>a</i>	<i>P</i> $\bar{1}$
<i>a</i> / nm	1.551 74(12)	1.505 72(19)
<i>b</i> / nm	1.551 74(12)	1.511 98(10)
<i>c</i> / nm	4.066 6(4)	1.610 58(10)
α / (°)		116.723(2)
β / (°)		107.987(2)
γ / (°)		98.020(2)
<i>V</i> / nm ³	9.791 9(14)	2.943 0(5)
<i>Z</i>	4	1
<i>D_c</i> / (g·cm ⁻³)	1.438	1.545
μ / mm ⁻¹	0.574	1.095
<i>R</i> ₁	0.074 3	0.039 4
<i>wR</i> ₂	0.175 2	0.116 8
GOF	1.112	1.033

DNA were further investigated by the fluorescence method. As the ligand HEx itself can luminesce, the fluorescence measurements were directly carried out by adding small aliquots of a certain concentration DNA stock to a 20 $\mu\text{mol}\cdot\text{L}^{-1}$ complex in buffer^[11].

1.4 Antibacterial tests

Antimicrobial activities of **1**, **2** and HEx as a reference substance, in 10% DMSO respectively, were evaluated using the agar diffusion test. The minimal inhibitory concentrations (MICs) of these compounds against six bacterial strains were determined.

2 Results and discussion

2.1 Crystal structures

X-ray diffraction study indicates that **1** is a mononuclear complex. As shown in Fig.1a, the central metal Ce(IV) ion is eight-coordinated by eight oxygen atoms from four Ex⁻ anions, forming a dodecahedron geometry. Each Ex⁻ anion, employing bidentate chelating coordination mode, bonds to Ce (IV) through the carbonyl oxygen (O3) and carboxylate oxygen (O1). The bond distance of Ce1-O_{carbonyl} (0.236 3 (4) nm) is slightly longer than the value of the Ce1-O_{carboxylate} (0.229 6(4) nm), which is consistent with the comparison result in other quinolone complexes^[12].

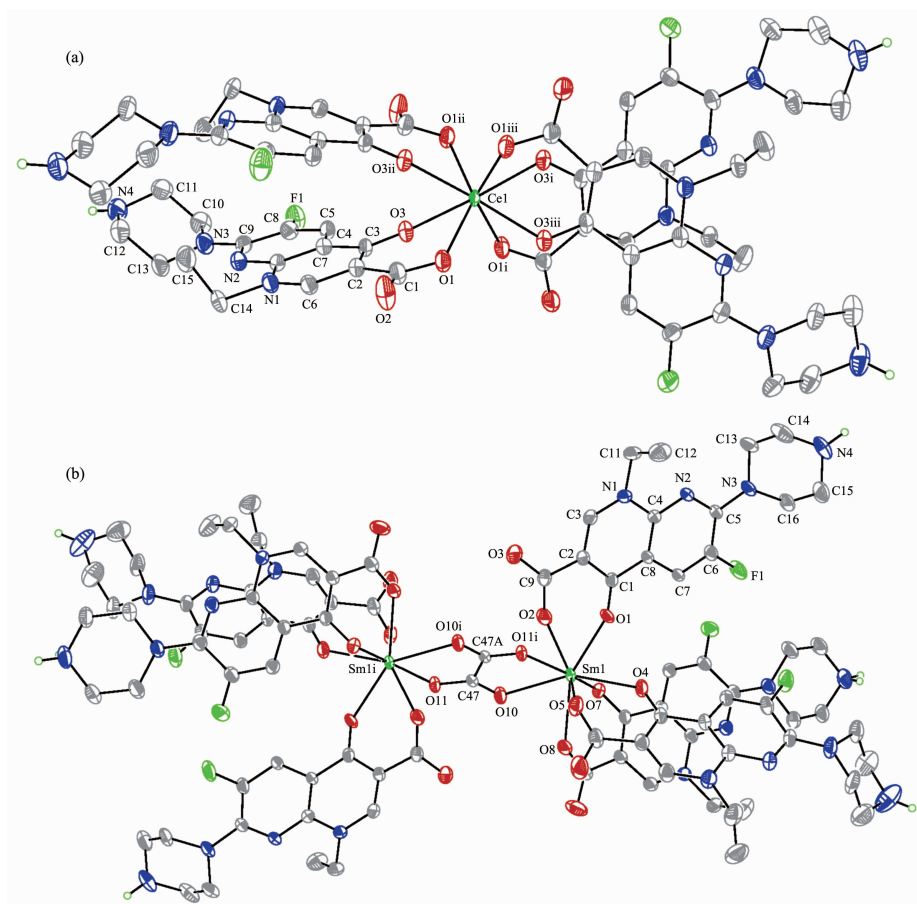
2 is an ox²⁻-bridged binuclear Sm(III) complex. Each Sm(III) ion, besides coordinating with two O atoms from one ox²⁻ anion, also coordinates with six oxygen atoms from two Ex⁻ anions and one HEx molecule, forming a square antiprism geometry. The ligands in **2**, similar to those in **1**, employ bidentate chelating coordination mode. The Sm-O bond distances, ranging from 0.236 2(3) to 0.244 5(3) nm, are unexceptional.

2.2 DNA binding

To investigate the binding of **1/2** to CT-DNA, the absorption spectra of **1/2** in the absence and presence of CT-DNA were screened at 25 °C. As shown in Fig. 2, with the addition of amounts of DNA, the MLCT band of **1** shifts from 276 to 282 nm and displays about 24% hypochromism (Fig.2a), and the MLCT band of **2** shift from 277 to 286 nm and yields 44% hypochromism (Fig.2b). These characteristics of red shift and hypochromism indicate that **1/2** binds with CT-DNA mostly using an intercalative mode^[13].

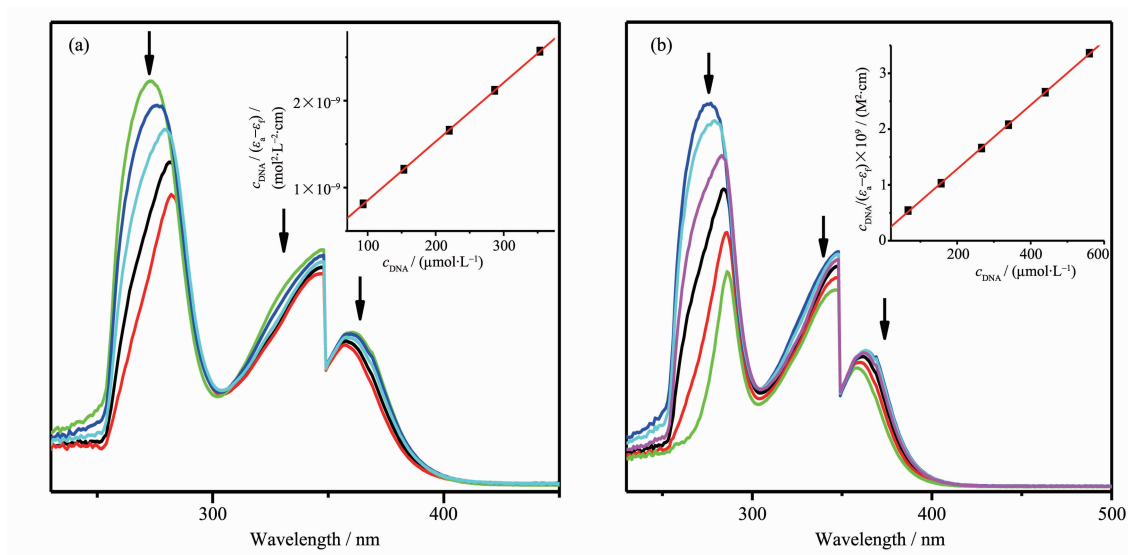
In order to quantitatively calculate the binding of **1** and **2** to CT-DNA, the intrinsic binding constants *K_b* of **1** and **2** were determined from the decay of the MLCT band absorbance (inset in Fig.2) and calculated using the following equation^[14].

$$c_{\text{DNA}}/(\varepsilon_a - \varepsilon_f) = c_{\text{DNA}}/(\varepsilon_b - \varepsilon_f) + 1/[K_b(\varepsilon_b - \varepsilon_f)]$$



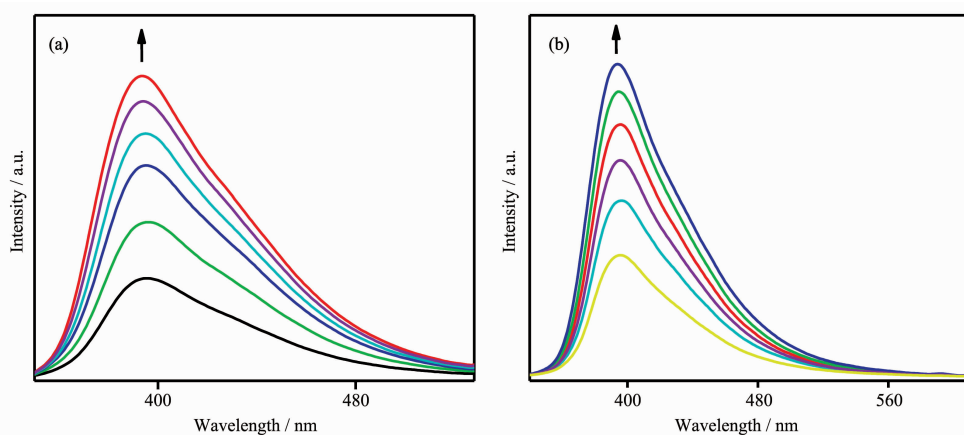
Thermal ellipsoids at 30% probability; for clarity, all lattice water molecules are omitted. Symmetry code: for **1**, i: $1-x, 1.5-y, z$; ii: $-0.25+y, 1.25-x, 1.25-z$; iii: $1.25-y, 0.25+x, 1.25-z$; for **2**, i: $1-x, 2-y, 1-z$

Fig.1 ORTEP drawing of **1** (a) and **2** (b) with atomic numbering scheme



(a) $c_{\text{complex 1}} = 20 \mu\text{mol} \cdot \text{L}^{-1}$, $c_{\text{DNA}}/c_{\text{complex 1}} = 0.0, 0.5, 1.0, 1.5$, and 2.0 ; (b) $c_{\text{complex 2}} = 20 \mu\text{mol} \cdot \text{L}^{-1}$, $c_{\text{DNA}}/c_{\text{complex 2}} = 0.0, 1.0, 2.0, 3.0, 4.0$ and 5.0 ; Arrows show the absorbance changes upon increasing DNA concentration. Inset: plots of $c_{\text{DNA}}/(\epsilon_a - \epsilon_f)$ vs c_{DNA} for the titration of DNA with complexes, \blacksquare , stand for experimental data points; solid line, linear fitting of the data

Fig.2 Absorption spectra of **1** (a) and **2** (b) in the presence of increasing amounts of CT-DNA with subtraction of the DNA absorbance



(a) $c_{\text{complex } 1} = 20 \mu\text{mol} \cdot \text{L}^{-1}$, $c_{\text{DNA}} = 10, 20, 40, 80, 160 \mu\text{mol} \cdot \text{L}^{-1}$; (b) $c_{\text{complex } 2} = 10 \mu\text{mol} \cdot \text{L}^{-1}$, $c_{\text{DNA}} = 10, 20, 40, 80, 160 \mu\text{mol} \cdot \text{L}^{-1}$; Arrows show the changes of the intensity upon increasing DNA concentration

Fig.3 Emission spectra of **1** (a) and **2** (b) in the presence of increasing amounts of CT-DNA

where c_{DNA} is the concentration of DNA in base pairs; the apparent absorption coefficients ε_a , ε_f and ε_b correspond to $A_{\text{obsd}}/c_{\text{complex}}$, the extinction coefficient for the free metal c_{complex} complexes and the extinction coefficient for the metal complexes in the fully bound form, respectively. In plots of $c_{\text{DNA}}/(\varepsilon_a - \varepsilon_f)$ vs c_{DNA} , K_b is given by the ratio of the slope to the intercept.

The determined intrinsic binding constants for **1** and **2** are 4.45×10^4 and $6.56 \times 10^4 \text{ mol}^{-1} \cdot \text{L}$ respectively. These values are comparable to those of complexes reported in literatures^[15].

The interactions of **1** and **2** with CT-DNA were further studied via emission spectra method. The results depicted in Fig.3 conspicuously illustrate the emission intensity of **1/2** increased steadily as increasing the amount of DNA, which implies **1/2** interacts with DNA mostly through an intercalative mode^[16-17]. This is quite consistent with the result concluded from the electronic absorption titration method.

2.3 Antibacterial tests

Table 2 shows the minimal inhibitory concentrations (MICs) of HEx, **1** and **2** against six bacteria respectively. The testing results indicate that these compounds tested are more active against Gram bacteria, but less active against fungi microbial (*Candida albicans*). Compared with the free HEx drug, the MIC value of **1** and **2** to any bacterial is smaller than the one of HEx, which reveals the **1** and **2**

exhibit better activities than that of the free ligand. This may be ascribed to the synergic effect between the metal ions and HEx.

Table 2 Minimal inhibitory concentrations (MICs, $\mu\text{g} \cdot \text{mL}^{-1}$) of HEx, **1**, and **2** for the following bacteria assayed

Microorganism	HEx	1	2
<i>Staphylococcus Aureus</i>	1.42	0.85	0.92
<i>b-hemolytic streptococcus</i>	5.65	3.54	4.87
<i>Streptococcus pneumoniae</i>	2.83	1.34	2.22
<i>Escherichia coliform</i>	0.36	0.13	0.28
<i>Pseudomona</i>	1.42	0.92	1.03
<i>Candida albicans</i>	1 446	897	1 025

3 Conclusions

Two rare earth complexes based on HEx have been synthesized and characterized. X-ray single crystal diffraction analysis indicates that **1** is a mononuclear complex and **2** is a binuclear complex. DNA binding investigations indicate that **1** and **2** can moderately bind with double-stranded DNA via intercalative mode. Antibacterial tests reveal that **1** and **2** have better activity against bacterial than the free ligand HEx.

References:

- [1] Hostetter A A, Chapman E G, DeRose V J. *J. Am. Chem. Soc.*, **2009**, *131*:9250-9257
- [2] Gao F, Chen X, Wang J Q, et al. *Inorg. Chem.*, **2009**, *48*:

- 5599-5601
- [3] HONG Xian-Lan(洪显兰), REN Jian-Min(任健敏). *Chinese J. Inorg. Chem.(Wuji Huaxue Xuebao)*, **2011**,**27**(4):785-790
- [4] Ni J Z. *Bioinorganic Chemistry of Rare Earth*. Beijing: Science Press, **2002**.
- [5] Wang Q, Yang Z Y, Qi G F, et al. *Eur. J. Med. Chem.*, **2009**, **44**:2425-2433
- [6] Well M, Naber-Kurt G, Kinzig-Schippers M, et al. *Int. J. Antimicrob. Agents*, **1998**,**10**:31-38
- [7] Klopman G, Wang S, Jacobs M R, et al. *Antimicrob. Agents Chemother.*, **1993**,**37**:1799-1806
- [8] Robles J, Martin Polo J, Álvarez-Valtierra L, et al. *Metal Based Drugs.*, **2000**,**7**:301-311
- [9] Sheldrick G M. *SADABS, Program for Empirical Absorption Correction of Area Detector Data*, University of Göttingen, Germany, **1996**.
- [10] Sheldrick G M. *SHELXS 97, Program for Crystal Structure Refinement*, University of Göttingen, Germany, **1997**.
- [11] Le Pecq J B, Paoletti C. *Anal. Biochem.*, **1996**,**17**:100-107
- [12] Efthimiadou E K, Psomas G, Sanakis Y, et al. *J. Inorg. Biochem.*, **2007**,**101**:525-535
- [13] Carter M T, Allen J. *J. Am. Chem. Soc.*, **1987**,**109**:7528-7530
- [14] Hertzberg R P, Dervan P B. *J. Am. Chem. Soc.*, **1982**,**104**: 313-315
- [15] PU Xiao-Hua(蒲小华), YANG Pin(杨频). *Chinese J. Inorg. Chem.(Wuji Huaxue Xuebao)*, **2010**,**26**(9):1567-1572
- [16] Zhou J, Wang L F, Wang J Y, et al. *J. Inorg. Biochem.*, **2001**,**83**:41-48
- [17] ZHOU Qing-Hua(周庆华), YANG Pin(杨频). *Acta Chim Sin.(Huaxue Xuebao)*, **2006**,**64**(8):95-100